

Fourth-order interference effects at large distances

J. G. Rarity and P. R. Tapster

Royal Signals and Radar Establishment, St. Andrews Road, Malvern, Worcestershire WR14 3PS, England

(Received 28 May 1991)

We present an experimental demonstration of a fourth-order interference effect first suggested by Franson [Phys. Rev. Lett. **62**, 2205 (1989)], where pair photons are directed to two separated Mach-Zehnder interferometers. Apparent nonlocal control of the output ports in which coincident photons are detected can be demonstrated. We show that this effect is present when one of the photons has passed through 170 m of multimode optical fiber. Such a system could form the basis of an interception-proof communication system.

PACS number(s): 42.50.Wm, 03.65.Bz, 42.25.Hz, 42.50.Dv

I. INTRODUCTION

Fourth-order interference occurring when pairs of photons are brought together in coincidence has been the subject of much study over the past few years [1–6]. The first experimental demonstration was obtained by superposing pair photons on a two-element detector [1]. The coincidence rate between elements oscillated with element separation. Although the detected effect was weak as a result of the finite detector size compared to the oscillation period, it is clearly nonclassical. It is also nonlocal in the sense that detection of a photon at one position strongly affects the possible positions of detection of its partner. Later work enhanced the visibility of the effect by recombining the photon pairs at a beam splitter [2–5] (allowing widely separated detectors to be used with improved optical efficiency). Nonlocal effects and violations of Bell's [7] inequality based on relative phase rather than polarization have recently been demonstrated in this type of apparatus [6].

The energy and momentum conservation inherent in the creation of two down-converted photons from one pump photon lead to a phase coherence of the combined pair-photon state, which extends beyond the coherence length of the individual pair beams. This coherence (or quantum-mechanical entanglement) is manifested when pair photons from parametric down conversion are input into two separate Mach-Zehnder interferometers [8]. Oscillations are seen in the coincidence rate as each interferometer path-length difference is scanned. Second-order interference effects (visible in the singles rates) are not seen when individual interferometer path-length differences are greater than the coherence length of individual pair-photon beams, but the coincidence oscillations remain as long as the separate path-length differences are equal to within the coherence length. With short-coincidence gate time, such an apparatus could exhibit oscillations with 100% visibility, thus allowing tests of local realistic theories to be performed. The maximum fringe visibility in most of these experiments has been limited to less than 50% [9,10], which has led to some discussion about whether the effects could be modeled by a classical source. Large oscillations in the coincidence rate (> 60% visibility) which were unequivocally nonclassical have been seen when the photons are input into the same Mach-Zehnder interferometer [11,12] and, more recently, using fast detectors and short-coincidence techniques [13].

As the pair photons are created simultaneously in the nondegenerate parametric down-conversion process [14], discriminant detection of pairs in high levels of background light can be achieved using narrow-coincidence gates. This led to the suggestion of a communication system for use in high backgrounds using photon-pair detection to code the signal [15]. Original realizations involved sending both photons of the pair down the communication channel, leading to a quadratic reduction of the signal-to-noise ratio with loss in the channel. We recently suggested [16] that an improved version of this apparatus would involve detection of one photon of the pair in the transmitter and sending a time stamp in the form of a standardized pulse using a conventional channel. The other photon traversing the high-background channel could be detected on using the time stamps to open the short-coincidence gate. The information was coded in the time delay between the time stamps and coincident photodetections in the receiver.

We show here that a more secure form of coding would be to use the nonlocal correlations occurring when identical Mach-Zehnder interferometers are placed in the transmitter and receiver. To this end we have constructed a down-conversion apparatus with pair photons directed to identical Mach-Zehnder interferometers and introduce into the signal arm, before the interferometer, a multimode fiber-optic cable of 170 m length. The relevant theory is described in Sec. II followed in Sec. III by a detailed description of this experiment.

We show here that a more secure form of coding would be to use the nonlocal correlations occurring when identical Mach-Zehnder interferometers are placed in the transmitter and receiver. To this end we have constructed a down-conversion apparatus with pair photons directed to identical Mach-Zehnder interferometers and introduce into the signal arm, before the interferometer, a multimode fiber-optic cable of 170 m length. The relevant theory is described in Sec. II followed in Sec. III by a detailed description of this experiment.

II. THEORY

A schematic apparatus is shown in Fig. 1. A pump beam with angular frequency ω_0 illuminates a parametric down-conversion crystal, and pair-photon beams are selected from the down-conversion cone using apertures placed to satisfy phase-matching conditions inside the crystal. The angular frequencies ω_s, ω_i of the signal and idler beams are set by the relative aperture positions and constrained to satisfy energy conservation at the crystal.

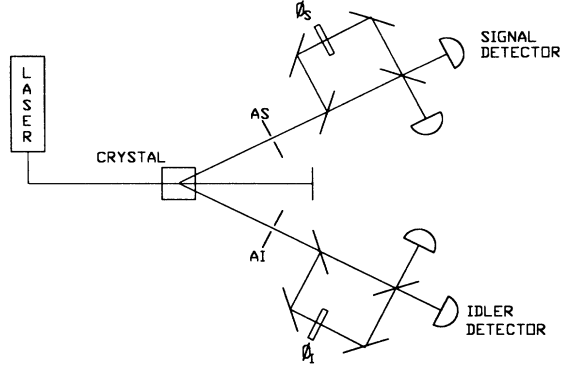


FIG. 1. Schematic of a two-photon interferometer. A short-wavelength laser illuminates a nonlinear crystal cut for nondegenerate parametric down conversion. Energy- and phase-matched photon pairs are selected by signal and idler apertures AS and AI and the pass through identical out-of-balance Mach-Zehnder interferometers to photon-counting detectors. Variable phase shifts ϕ_s and ϕ_i are introduced in the long arms of the interferometers.

Signal and idler arms of the apparatus contain identical Mach-Zehnder interferometers with path-length difference ΔT and phase plates introducing small phase shifts ϕ_s, ϕ_i . In a simplistic analysis we assume ideal detectors, a coincidence gate width Δt much narrower than ΔT , and 50-50 beam splitters. The two-photon state is then represented at the detectors by the entangled state

$$\Psi_{si} = \frac{1}{\sqrt{2}} (|1_{\text{long}}\rangle_i |1_{\text{long}}\rangle_s e^{i(\phi_i + \phi_s)} e^{i\Delta T(\omega_i + \omega_s)} + |1_{\text{short}}\rangle_i |1_{\text{short}}\rangle_s), \quad (1)$$

where $|1\rangle_{s,i}$ denotes a one-photon state in a signal-idler arm of the apparatus, the subscripts *long* and *short* denote propagation via the long and short paths through the interferometer, and the phase shifts incorporate any phase changes occurring on reflection. Being a superposition of a *long, long* two-photon state with a *short-short* two-photon state, this wave function directly expresses the uncertainty in time of the emission of the photon pair. Coherence between the two possible emission times is ensured when the pump laser has a constant frequency ω_0 (i.e., a long coherence length as compared to ΔT) and when energy conservation is strictly applied in the relationship $\omega_i + \omega_s \equiv \omega_0$.

The probability P_{si} of seeing a photon in the signal arm coincident with an idler arm photodetection is then given by

$$P_{si} = \eta_s \eta_i \langle \Psi | \hat{a}_i^\dagger \hat{a}_s^\dagger \hat{a}_s \hat{a}_i | \Psi \rangle, \quad (2)$$

where η_s and η_i are detector efficiencies and \hat{a}_s and \hat{a}_i are annihilation operators for photons in the signal and idler beams, respectively. Consequently,

$$P_{si} = \frac{1}{2} \eta_s \eta_i [1 + \cos(\phi_i + \phi_s + \omega_0 \Delta T)]. \quad (3)$$

The striking fact about this result is that the probability of coincident detection of two apparently separate photons can be modulated with 100% certainty using either of the widely separated phase plates. These apparent nonlocal effects can be used to demonstrate violations of local realistic theories or Bell inequalities [7]. This simplified theory assumes ideal detection and narrow-coincidence gates $\delta t \ll \Delta T$, ideal 50-50 beam splitters, and ignores the finite bandwidth of pump and down-converted photons. In a real experiment we measure a coincidence rate which is proportional to the integral of the pair-photon detection probability over a finite gate width Δt ,

$$C(\Delta T) = \eta_s \eta_i \int_{-\Delta t/2}^{+\Delta t/2} d\tau \langle \Psi | \hat{A}_s^\dagger(t) \hat{A}_i^\dagger(t+\tau) \times A_i(t+\tau) A_s(t) | \Psi \rangle, \quad (4)$$

where the broadband photon-annihilation operator $\hat{A}^\dagger(t)$ at time t (proportional to the electric-field operator) is given by an integration over single-mode annihilation operators

$$\hat{A}_s^\dagger(t) = \int d\omega_s \hat{a}_s(\omega_s) e^{i\omega_s t}, \quad (5)$$

and similarly with subscript s replaced by i . The operator \hat{a}_s at the detectors can be expressed in terms of the operators at the crystal \hat{a}_{cs} by projecting back through the interferometer,

$$\hat{a}_s(\omega_s) = \hat{a}_{cs}(\omega_s) (T + R e^{i(\omega_s \Delta T_s)}), \quad (6)$$

where R and T are intensity reflection and transmission coefficients at the beam splitters (all beam splitters will be assumed identical in this analysis). Again, the idler beam case is obtained by replacing subscripts s and cs by ci . The phase change ϕ_s would not normally be consistent with changing wavelength; thus it has been subsumed into ΔT_s .

The wave function of the light produced at the crystal is more accurately represented by a superposition of vacuum and a small amount of two-photon light [10],

$$\Psi(t) = (1 - E_0^2 \alpha^2)^{1/2} |\text{vac}\rangle_{cs} |\text{vac}\rangle_{ci} + E_0 \alpha \int d\omega f(\omega) \left| \frac{\omega_0}{2} + \omega \right\rangle_{cs} \left| \frac{\omega_0}{2} - \omega \right\rangle_{ci}, \quad (7)$$

in the case where spontaneous parametric fluorescence dominates any stimulated pair production. We include here a down-conversion quantum efficiency factor α^2 and pump mean field E_0 with $|E_0|^2$ measured in pump photons per second falling on the crystal. The spectra of the two photons, $f(\omega)$, is limited primarily by apertures [5] or external filters. ω is defined by energy conservation when $\omega_s = \omega_0/2 + \omega$, $\omega_i = \omega_0/2 - \omega$. The down-converted light need not be centered on $\omega_0/2$. For the purposes of

this analysis, we will assume a Gaussian form for the filter function,

$$f(\omega) = a \exp \left[-\frac{(\omega_c - \omega)^2}{2\sigma^2} \right], \quad (8)$$

with $1/e^{1/2}$ width σ , and signal and idler center frequencies defined by $\omega_{s0} = \omega_0/2 + \omega_c$, $\omega_{i0} = \omega_0/2 - \omega_c$. The normalization constant a is set by $2\pi \int d\omega |f(\omega)|^2 = 1$.

Equations (4)–(8) can be combined and simplified using the orthogonality relations typified by

$$\begin{aligned} \beta \langle \omega | \hat{a}_{\beta'}(\omega') \hat{a}_{\gamma'}^\dagger(\omega'') | \omega''' \rangle_{\gamma} \\ = \delta(\omega' - \omega) \delta(\omega'' - \omega''') \delta_{\gamma\gamma'} \delta_{\beta\beta'}, \quad (9) \end{aligned}$$

with $\gamma, \gamma', \beta, \beta'$ given by *cs* or *ci*. The resulting coincidence rate has the form

$$\begin{aligned} F(\Delta t, \Delta T_s, \Delta T_i) &= 2\pi a^2 \int_{-\Delta t/2}^{+\Delta t/2} d\tau \{ \exp[-\sigma^2(\tau + \Delta T_s)^2] + \exp[-\sigma^2(\tau + \Delta T_i)^2] \} \\ &\equiv 2, \quad \Delta t \gg \Delta T_{i,s} \gg \sigma^{-1}, \\ &\equiv 0, \quad \Delta T_{i,s} \gg \Delta t \gg \sigma^{-1}, \end{aligned}$$

disappears when the coincidence circuitry can resolve long-short events.

The coherence of the pump beam can be included simply by integrating the coincidence rate over the pump power spectrum $\Gamma(\omega_0)$. When we assume a Gaussian form for the laser spectrum (this is a typical envelope function for a multimode gas laser) gate resolving time $\Delta t \gg \Delta T_{s,i}$ and 50-50 beam splitters ($R = T = 0.5$),

$$\begin{aligned} C(\Delta t) &= \frac{1}{4} \eta_s \eta_i E_0^2 \alpha^2 \{ 1 + \frac{1}{2} \exp[-\sigma^2(\Delta T_s - \Delta T_i)^2] \\ &\quad \times \exp(-\sigma'^2 \Delta T^2) \\ &\quad \times \cos(\omega_{s0} \Delta T_s + \omega_{i0} \Delta T_i) \}, \quad (12) \end{aligned}$$

where laser center frequency is ω_{00} with $1/e$ spectral width σ' and signal and idler center frequencies defined by $\omega_{s0/i0} = \omega_{00}/2 \pm \omega_c$. $\Delta T = (\Delta T_s + \Delta T_i)/2$ is the mean path-length difference, and interference effects disappear as this path-length difference exceeds the coherence time of the pump beam, $\sim \sigma'^{-1}$. Because of the poor time resolution of typical coincidence gates, we expect Eq. (12) to describe most realizable experiments. The visibility of the oscillation is limited to less than 50%. In principle, such a result could be obtained by assuming a classical phase correlation between the pair-photon beams. However, related experiments over shorter separations have shown that the 50% visibility criterion can be exceeded [6,11,13], confirming the need for a fully quantum-mechanical theory as given above.

III. EXPERIMENT

A diagram of the apparatus is shown in Fig. 2. A lithium iodate crystal pumped by a helium-cadmium laser

$$\begin{aligned} C(\Delta t) &= \eta_s \eta_i E_0^2 \alpha^2 \left[R^4 + T^4 + R^2 T^2 F(\Delta t, \Delta T_s, \Delta T_i) \right. \\ &\quad \left. + 2R^2 T^2 \exp \left[\frac{-\sigma^2(\Delta T_s - \Delta T_i)^2}{4} \right] \right. \\ &\quad \left. \times \cos(\omega_{s0} \Delta T_s + \omega_{i0} \Delta T_i) \right], \quad (10) \end{aligned}$$

when detectors are placed as shown (Fig. 2). We have assumed that $\Delta t, \Delta T_{s,i} \gg \sigma^{-1}$, thus allowing the time-integration limits to be approximated by $\pm \infty$ where appropriate. The third term contains the oscillating interference component and is only visible when the interferometers are matched to within the coherence lengths of the down-converted photons ($\Delta T_s - \Delta T_i < \sigma^{-1}$). The second term reflects the coincidence rate from $|1_{\text{short}}\rangle_i |1_{\text{long}}\rangle_s$ and $|1_{\text{long}}\rangle_i |1_{\text{short}}\rangle_s$ photon pairs. The function

operating at 441.6-nm wavelength was used as a source of photon pairs. The crystal axis was tilted to produce 883.2-nm wavelength pair beams separated by an angle of about 30°. Small (~ 3 mm diameter at 600 mm from the crystal) apertures were used to select the beams. The pump beam was unfocused (~ 2 mm diameter), and hence these apertures were multimode. Initially, photon-counting detectors covered by interference filters were placed behind the apertures, and the coincidence rate between the detectors was maximized by moving the apertures to the optimum phase-matching angles. At normal incidence the filter center wavelengths were 890 and 900

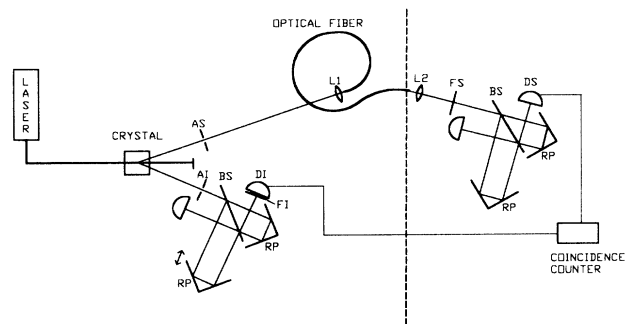


FIG. 2. Experimental setup. A helium-cadmium laser illuminates a crystal of lithium iodate. Down-converted beams are selected by apertures AS and AI in combination with filters FS and FI placed in front of the signal and idler detectors DS and DI. The signal beam is launched into a multimode optical fiber using a microscope lens (L1) and collimated by a second lens (L2) at the output. The Mach-Zehnder interferometers are constructed from single beam splitters (BS) and retroreflecting prisms (RP), one of which can be moved on a stepper-motor-driven micropositioner.

nm. Thus they were tilted to shift the center wavelengths closer to 883.2 nm, and in a final optimization of the coincidence rate, this tilt was further adjusted. A Mach-Zehnder interferometer was then placed in the idler arm of the apparatus between the aperture and detector. In the signal arm a microscope objective [$\times 10$, 0.25 numerical aperture (NA)] was placed behind the aperture to launch light into a multimode fiber (0.23 NA) of length 170 m. Light from the fiber end is collimated by another microscope lens and launched into a second Mach-Zehnder interferometer. Photon-counting detectors are placed to detect the light output from each interferometer. A simplified form of the Mach-Zehnder interferometer is used involving a single beam splitter and retroreflecting prisms (see Fig. 2). One retroreflecting prism is mounted on a stepper-motor-driven translational stage with 0.1- μm resolution to allow adjustment of the path difference. When detectors are placed as shown, all paths through the interferometer involve one reflection and one transmission at the beam splitter. In this case the ideal (50%) visibility predicted by Eq. (12) holds for arbitrary beam splitters with mean coincidence rate reduced by a factor $16(R^2T^2)$ (≈ 0.92 here as $R \approx 0.4$, $T \approx 0.6$). The interferometers were both calibrated to zero-path-length differences by finding white-light (10-nm-bandwidth filtered tungsten bulb) fringes and then carefully adjusted to identical 2-mm-path-length differences. At this point no white-light fringes could be seen. The down-converted photons have similar bandwidths, and scanning the interferometer around the 2-mm-path-length-difference position did not produce any oscillations in the photoelectron-count rate. With 10-nm-bandwidth filters in front of the detectors, the signal channel singles rate was around 30 kilocounts per second, including a dark count of some 10 kilocounts/s. The idler channel count rate was about 70 kilocounts/s, again with significant background contribution. The coincidence rate was measured by delaying the idler channel counts in a pulse generator using a 10-ns-gate-time multichannel coincidence counter. The background coincidence rate due to random overlap of pulses in the gate time was thus about 20 counts/s, while the coincidence peak after background subtraction showed some 600 coincidences/s (on average). The average coincidence rate predicted by Eq. (12) and the above is

$$C(\Delta t) = \frac{0.92}{4} \eta_s \eta_i E_0^2 \alpha^2, \quad (13)$$

and we expect singles rates in the detectors to be given by $0.5\eta_{s,i}E_0^2\alpha^2$ with any propagation losses lumped into the effective quantum efficiencies $\eta_{s,i}$. Our results thus suggest that effective detector efficiencies were $\eta_s \approx 0.02$ and $\eta_i \approx 0.06$. Fiber losses were about a factor of 3.

The path-length difference in one of the Mach-Zehnder interferometers was changed in 0.2- μm steps using the computer-controlled translation stage and 5-s measurements of the coincident rate were made over a 100- μm range of travel around the equal 2-mm-path-length-difference position.

A section of the collected data is shown in Fig. 3. Clearly, the oscillation has a period close to 883 nm, but

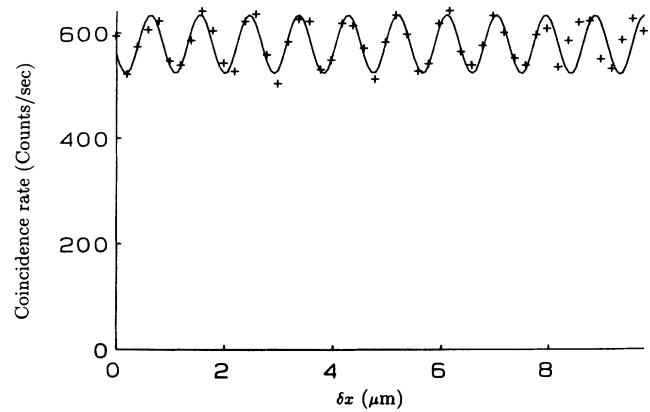


FIG. 3. Coincidence rate measured as a function of path-length difference $\delta x = c\Delta T$ over a 10- μm range close to the equivalent 2-mm-path-length-difference point.

the visibility is somewhat below the expected value of 0.5. The full result is shown in Fig. 4 along with a computer fit to the data using an equation of the form given in Eq. (12). The floating parameters were determined to be the following: mean coincidence rate = 576 counts/s, visibility = 0.083, periodicity = 0.896 μm , and Gaussian envelope width $2c/\sigma = 50.8 \mu\text{m}$ ($\sigma = 1.18 \times 10^{13}$ rad/s). The filters used had a full width at half maximum bandwidth of 10

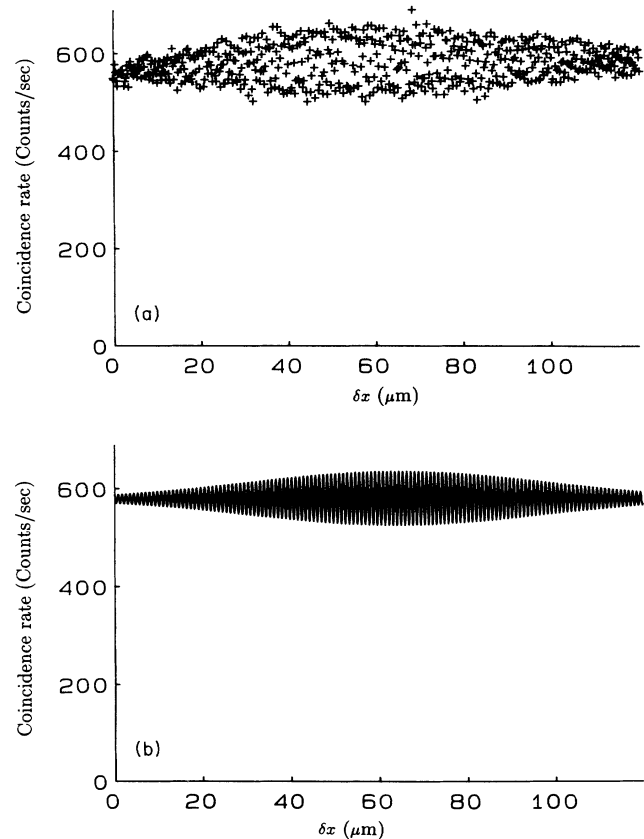


FIG. 4. (a) Coincidence rate measured as a function of path-length difference $\delta x = c\Delta T$ over a 100- μm range around the equivalent 2-mm-path-length-difference point. (b) Theoretical fit to the data using an equation of the form shown in Eq. (12).

nm, which corresponds to a bandwidth of $\sigma = 1.42 \times 10^{13}$ rad/s, agreeing reasonably with the fit. The slightly high measured wavelength reflects the slight imbalance in filter center frequencies. The visibility is underestimated because of the fitting procedure, which tries to fit a single sine wave to the data having phase fluctuations caused by drive nonlinearity at the submicrometer level. Fitting a short section of data as in Fig. 3 leads to a visibility of 11.3%. This is still well below 50%, which could be interpreted in terms of a short-coherence-length pump beam [cf. Eq. (12)], but we presume it is more associated with spatial averaging in the interferometers and mode scrambling in the fiber. Individually measured interferometers showed interference fringes with about 75% visibility when illuminated with both white light and helium-neon laser light.

IV. DISCUSSION

We expect that the low visibility will be improved by use of better optics in the interferometers, but with the present detector resolutions, it is still limited to 50%. One can think of classical sources that could mimic this behavior [9] with similar visibilities. Taken in isolation, this experiment does not prove absolutely that the entangled state exists over the 170-m detector separation. Recent work [21], however, has shown that given the highly time correlated nature of the photon pairs determined in independent experiments [22], a classical description of the experiment is inadequate.

To achieve higher visibilities the second term in Eq. (10) must be reduced to zero. For this, the combined coincidence gate Δt and detector jitter must be shorter than the time difference ΔT . This is technically feasible using detectors with < 100-ps jitter [17], time-to-height converters, a single-mode pump laser, and path-length

differences of a few centimeters. Recently, such an experiment has been successfully performed using a coincidence time resolution of 500 ps [13] (at small separations between signal and idler beams). If correlations close to 100% are achieved, then applications in quantum cryptography systems [18] will be possible.

The delay between emission and arrival at the signal-beam interferometer is about 1 μ s. Rapid adjustment of the phase plate in this arm (on time scales shorter than 1 μ s) would allow delayed-choice tests of local realistic theories [19]. It is also of academic interest to verify whether nonclassical correlations are retained over large distances and whether these effects can be used to test the assumption of linearity in quantum mechanics.

In conclusion, we have demonstrated pair-photon interference in interferometers separated by 170 m of optical fiber. Such effects could form the basis of a secure communication system [20] given the requirement that interferometer path-length differences have to be matched to within a few micrometers (the coherence-length set by the single-photon bandwidth), while actual path-length differences can be up to a few centimeters. An eavesdropper intercepting the system at the dashed line shown in Fig. 2 would see Poisson random-pulse trains in both signal and idler paths and in the coincidences between them. The remote interferometer can be thought of as a key which has to be set to the correct value (path-length difference) before information (modulation of the coincidence rate) can be received.

ACKNOWLEDGMENTS

This work is supported in part by the European Economic Community Esprit scheme, Grant No. BRA:3186.

-
- [1] R. Ghosh and L. Mandel, *Phys. Rev. Lett.* **59**, 1903 (1987).
 - [2] J. G. Rarity and P. R. Tapster, in *Photons and Quantum Fluctuations*, edited by E. R. Pike and H. Walther (Hilger, London, 1988), p. 122; *J. Opt. Soc. Am. B* **6**, 1221 (1989).
 - [3] C. K. Hong, Z. Y. Ou, and L. Mandel, *Phys. Rev. Lett.* **59**, 2044 (1987).
 - [4] Z. Y. Ou and L. Mandel, *Phys. Rev. Lett.* **61**, 54 (1988).
 - [5] J. G. Rarity and P. R. Tapster, *Phys. Rev. A* **41**, 5139 (1990).
 - [6] J. G. Rarity and P. R. Tapster, *Phys. Rev. Lett.* **64**, 2495 (1990).
 - [7] J. S. Bell, *Physics* **1**, 19 (1964).
 - [8] J. D. Franson, *Phys. Rev. Lett.* **62**, 2205 (1989).
 - [9] P. G. Kwiat, W. A. Vareka, C. K. Hong, H. Nathel, and R. Y. Chiao, *Phys. Rev. A* **41**, 2910 (1990).
 - [10] Z. Y. Ou, X. T. Zou, L. J. Wang, and L. Mandel, *Phys. Rev. Lett.* **65**, 321 (1990).
 - [11] J. G. Rarity, P. R. Tapster, E. Jakeman, T. Larchuk, R. A. Campos, M. C. Teich, and B. E. A. Saleh, *Phys. Rev. Lett.* **65**, 1348 (1990).
 - [12] Z. Y. Ou, X. Y. Zou, L. J. Wang, and L. Mandel, *Phys. Rev. A* **42**, 2957 (1990).
 - [13] J. Brendel, E. Mohler, and W. Martienssen, *Phys. Rev. Lett.* **66**, 1142 (1991).
 - [14] D. C. Burnham and D. L. Weinberg, *Phys. Rev. Lett.* **25**, 84 (1970).
 - [15] C. K. Hong, S. Friberg, and L. Mandel, *Appl. Opt.* **24**, 3877 (1985).
 - [16] S. Seward, J. G. Walker, J. G. Rarity, and P. R. Tapster, *Quantum Opt.* **3**, 201 (1991).
 - [17] S. Cova, M. Laciata, M. Ghioni, G. Ripamonti, and T. A. Louis, *Rev. Sci. Instrum.* **60**, 1104 (1989).
 - [18] A. Ekert, *Phys. Rev. Lett.* **67**, 661 (1991).
 - [19] A. Aspect, J. Dalibard, and G. Roger, *Phys. Rev. Lett.* **49**, 1804 (1982).
 - [20] U. K. patent application No. 901873.9 (1991).
 - [21] J. D. Franson, *Phys. Rev. Lett.* **67**, 290 (1991).
 - [22] S. Friberg, C. K. Hong, and L. Mandel, *Phys. Rev. Lett.* **54**, 2011 (1985).